Varieties of Stable Vortical Solitons in Ginzburg-Landau Media with Radially Inhomogeneous Losses

V. Skarka,[1,2] N. B. Aleksić,[2] H. Leblond,[1] B. A. Malomed,[3] and D. Mihalache[4]

[1]*Laboratoire de Photonique d'Angers, EA 4464, Université d'Angers, 2 Boulevard Lavoisier, 49045 Angers Cedex 01, France*
[2]*Institute of Physics, University of Belgrade, 11000 Belgrade, Serbia*
[3]*Department of Physical Electronics, Faculty of Engineering, Tel Aviv University, Tel Aviv 69978, Israel*
[4]*Horia Hulubei National Institute for Physics and Nuclear Engineering, 407 Atomistilor, Magurele-Bucharest, 077125, Romania*

(Received 18 July 2010; published 15 November 2010)

Using a combination of the variation approximation and direct simulations, we consider the model of the light transmission in nonlinearly amplified bulk media, taking into account the localization of the gain, i.e., the linear loss shaped as a parabolic function of the transverse radius, with a minimum at the center. The balance of the transverse diffraction, self-focusing, gain, and the inhomogeneous loss provides for the hitherto elusive stabilization of vortex solitons, in a large zone of the parameter space. Adjacent to it, stability domains are found for several novel kinds of localized vortices, including spinning elliptically shaped ones, eccentric elliptic vortices which feature double rotation, spinning crescents, and breathing vortices.

DOI: 10.1103/PhysRevLett.105.213901 PACS numbers: 42.65.Tg, 42.65.Sf, 47.20.Ky

Introduction and the model.—Self-collimated and self-guided light beams, organized as spatial solitons in bulk media, are subjects of great interest [1]. In addition to their significance for fundamental studies, spatial solitons can find applications to the design of all-optical data-processing schemes. In particular, laser systems may run on dissipative optical solitons, which are described by the complex Ginzburg-Landau equations (CGLEs), typically with the cubic-quintic (CQ) nonlinearity, taking into account the saturable nonlinear gain [2]. Crucially important to the applications is the stability of dissipative solitons. Families of stable spatial solitons in two transverse dimensions (2D) exist in materials characterized by a saturable nonlinearity that compensates the diffraction [1,3]. The additional condition of the balance between losses and gain reduces the family to isolated solutions, one of which may be stable as an *attractor* [4,5].

The complexity of the CGLEs does not admit exact solutions, even in an implicit form, with rare exceptions [5–7]. Nevertheless, an analytical approximation, which provides clues to finding dissipative solitons in the numerical form, has been developed in the form of the variational approach (VA) adopted for dissipative systems [8]. Parameter domains where 2D and 3D solitons are stable in the CQ-CGLE and related models have been outlined by means of this method [8,9].

Objects of fundamental significance which remained elusive in the studies of dissipative solitons are solitary vortices. In previous works, such vortices were found to be stable only in the presence of the diffusion, which occurs in other physical media, but does not appear in laser systems [9,10], nor in dissipative models of Bose-Einstein condensates (BECs) [11]. The stabilization of multipeak patterns carrying vortical phase patterns was demonstrated by periodic potentials that may be created in the laser cavity [9]. Nevertheless, the most fundamental circular (''crater-shaped'') localized vortices were not found yet as stable objects in models of optical media. In this Letter, we report (for the first time, to our knowledge) *stable* fundamental vortical modes in a physically relevant model where the stabilization is provided by an axisymmetric modulation of the linear loss, with a minimum at the center. In the experiment, the loss modulation may be induced by a localized gain which partly compensates the uniform loss (an ''iceberg of gain'' submerged into the ''sea of loss''). In fact, the gain applied to a laser cavity is always localized, due to the finite width of the pumping beam. Besides the optical media, similar modulated loss profiles can be engineered in BEC, where they help to support various matter-wave modes [11].

We also demonstrate that, when the axisymmetric vortices lose their stability, they give rise to other novel types of vorticity-carrying modes. These are spinning elliptically deformed vortices, eccentric elliptic vortices which feature spinning and precessing, revolving crescents, and breathing vortices. Thus, the use of the 2D ''iceberg-shaped'' gain profile opens the way to the previously inaccessible class of *stable* vortical modes in dissipative optical media.

We adopt the $(2+1)D$ form of the CQ-CGLE governing the evolution of the optical field in the bulk medium, $E(z, x, y)$, along axis z, and the diffraction in the transverse plane [2,4]:

$$iE_z + (1/2)(E_{xx} + E_{yy}) + (1 - i\varepsilon)|E|^2E - (\nu - i\mu)|E|^4 \times E = -ig(r)E, \qquad r \equiv \sqrt{x^2 + y^2}, \tag{1}$$

where positive coefficients ν, ε, and μ account for the saturation of the Kerr nonlinearity, cubic gain, and quintic

loss, respectively, and the linear-loss coefficient is modulated along the radial coordinate, $g(r) = \gamma + Vr^2$, with γ, $V > 0$. Note that the limit form of a similar 1D model, with the linear gain concentrated at a single "hot spot" (approximated by the delta function) and cubic nonlinearity, admits exact stable solutions for pinned solitons [6].

The variation approximation.—First, we aim to obtain approximate analytical results, using the VA technique [8]. We adopt the ansatz for the vortex soliton with topological charge 1,

$$E = \frac{A_* A r}{R_* R} \exp\left(-\frac{r^2}{2R_*^2 R^2} + i\frac{Cr^2}{R_*^2} + i\theta + i\Psi\right), \quad (2)$$

where θ is the angular coordinate, normalizing factors are $A_* = 3/(2\sqrt{2})$ and $R_* = 16/9$, while variation parameters are amplitude A, radius R, radial chirp C, and phase Ψ. The total power corresponding to ansatz (2) is $P \equiv 2\pi \int_0^\infty |E(r)|^2 r dr = P_* A^2 R^2$, with $P_* \equiv \pi A_*^2 R_*^2$. After straightforward calculations, the VA leads to the system of evolution equations:

$$\frac{dA}{dz} = \frac{A}{R_*^2}\left(\frac{5}{2}\varepsilon A^2 - 2\mu A^4 - 2C\right) - A(\gamma + R_*^2 V R^2), \quad (3)$$

$$\frac{dR}{dz} = \frac{R}{R_*^2}\left(2C - \frac{\varepsilon}{2}A^2 + \frac{\mu}{2}A^4 - R_*^4 V R^2\right), \quad (4)$$

$$\frac{dC}{dz} = \frac{1}{R_*^2}\left(\frac{1}{2R^4} - \frac{A^2}{2R^2} + \frac{\nu A^4}{2R^2} - 2C^2\right). \quad (5)$$

Steady-state solutions are obtained as fixed points (FPs) of Eqs. (3)–(5), in the shaded area displayed in Fig. 1 (outside of this area, there is only solution $A = 0$). For small chirp, it follows from Eq. (5) that the width of the stationary state depends only on its amplitude, $R^2 = (A^2 - \nu A^4)^{-1}$, as in conservative systems. In the first approximation, the small chirp, which makes the dissipative solitons different from their conservative counterparts, is obtained from Eq. (4): $C = A^2(\varepsilon - \mu A^2)/4 + R_*^4 V/[2A^2(1 - \nu A^2)]$.

Further analytical consideration of the FP solutions reveals that they give rise to two different amplitudes A, as shown in the inset to Fig. 1. As per general principles of the analysis of dissipative systems, the solution with larger A may be stable, while its counterpart with smaller A corresponds to an unstable separatrix between the two attractors [5]—the stable vortex and trivial state, $E = 0$. The solution with larger A is characterized by $C < 0$, which also is a necessary stability condition for the steady state [8]. The stability of the FPs corresponding to the larger root for A was verified through the computation of eigenvalues for small perturbations.

Numerical results.—The full stability area for the vortex solitons (marked "stable" in Fig. 1) was identified by means of direct simulations of Eq. (1), using the VA-produced ansatz as the input. The VA predicts the qualitative shape of the area correctly, although overestimating its size. A typical example of the fast formation of a stable vortex (which completes by $z = 20$, i.e., after passing $\lesssim 4$ diffraction lengths) is displayed in Fig. 2.

In the "filamentation" region in Fig. 1, the modulation instability breaks the vortex into two segments, at $z \sim 1000$ (closer to the stability border, this distance increases to $z \sim 3000$). This outcome of the evolution is explained by the fact that, in this region, the total power of the vortex (P) falls below the breakup threshold; cf. similar instability scenarios reported in Refs. [9–12].

In region E separating the stability and breakup domains in Fig. 1, P exceeds the breakup threshold, hence the vortex does not split. However, in this region the evolution leads to squeezing the circular vortex into an *elliptic rotating* one, which remains stable. For instance, in Fig. 3, the circular vortex persists until $z = 3700$. The further evolution,

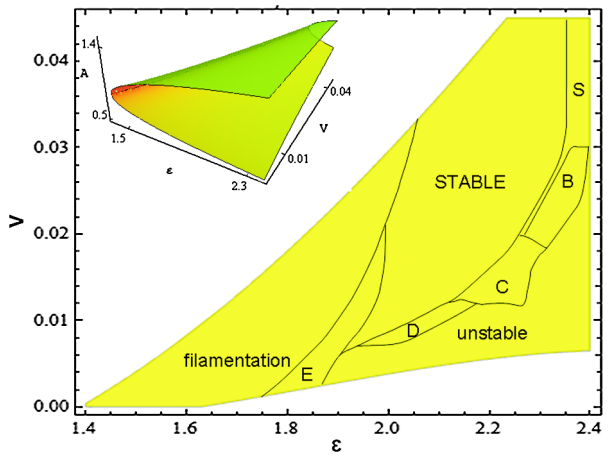

FIG. 1 (color online). Stability regions of vortex solitons in plane (ε, V) of the loss-modulation parameters. In this figure and below, other coefficients in Eq. (1) are $\gamma = 0.29$, $\mu = 1.4$, $\nu = 0.4$. The VA predicts the stability in the shaded area, and the corresponding amplitude displayed in the inset.

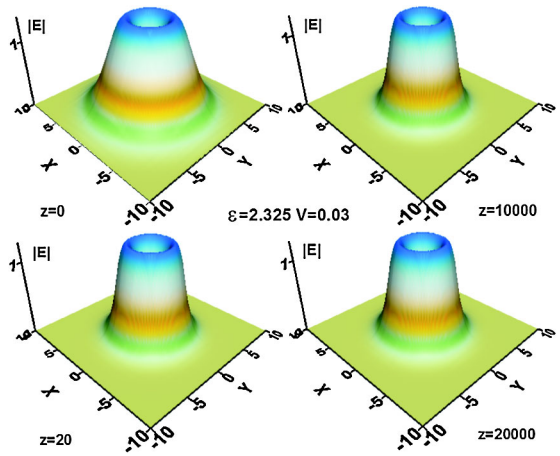

FIG. 2 (color online). The self-trapping of a stable vortex from the input predicted by the VA, at $\varepsilon = 2.325$ and $V = 0.03$.

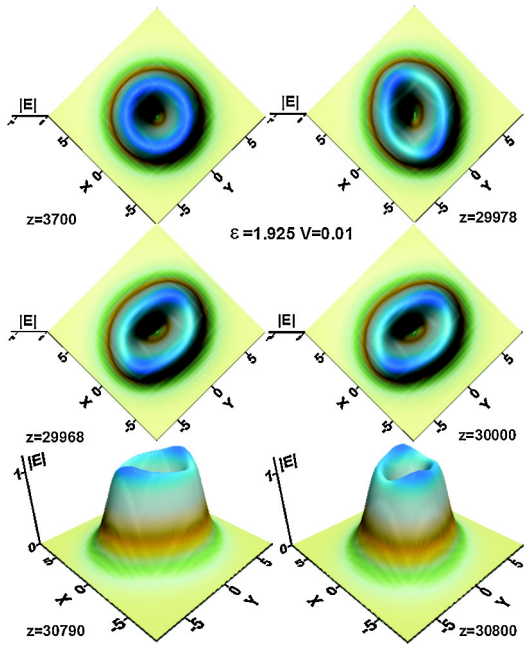

FIG. 3 (color online). The self-trapping of a stably rotating elliptic vortex. The configurations displayed at $z = 29\,968$ and $z = 30\,000$ correspond to the rotation of the ellipse by 180°. Images in the bottom row display the established shape of the elliptic vortex.

lasting for $\Delta z \approx 200$, ends up with the transition into a *stable* elliptic soliton of a larger amplitude, which revolves with a constant period, $Z \approx 32$. Its profile features a "volcanic" shape, with an undulate "crater" (see the bottom row). This is a novel type of vorticity-carrying solitons in dissipative media. Note that elliptically deformed vortices were observed in a conservative nonlocal optical medium [13], and they were studied theoretically in diverse settings [14], but in those cases the ellipticity was imposed by anisotropic boundaries, while here the transition to the elliptic shape is generated *intrinsically*. Rotating solitons of other types ("dipole propellers") were also predicted and demonstrated in conservative media, but in those cases the rotation was imparted, rather than spontaneous [15].

In the right-bottom ("unstable") region of Fig. 1, the vortices suffer destruction after the propagation distance measured in hundreds of units (closer to the border of region E, this distance extends to thousands). Four regions D, C, B, and S, which separate the stable and unstable regions in Fig. 1, feature other remarkable vortical patterns. In region D, the stable elliptic vortex spontaneously becomes *eccentric*. As shown in Fig. 4, it develops the eccentricity after $z = 8500$, and after $z = 14\,000$ it slips out from the central position and starts precessing around it, thus featuring *double rotation* (the precession and spinning) in the same direction, with an apparently locked period ratio, $216/54 = 4$, which may be caused by a nonlinear parametric resonance in the original spinning elliptic

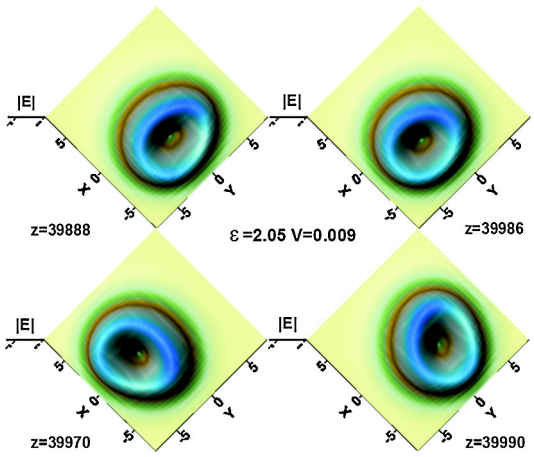

FIG. 4 (color online). A stable *eccentric* spinning vortex, which orbits around the center.

vortex. The eccentric elliptic vortices remain stable in the course of this complex motion.

Another variety of spontaneously deformed rotating vortices occupies region C in Fig. 1. As shown in Fig. 5, after $z = 660$ the circular symmetry is broken by generating a *crescent-shaped* vortex, which fills a half of the original circle. The crescent rotates around the center, with period $Z \approx 12$ (see panels in Fig. 5 for $z = 25\,988$ and $z = 26\,000$). Stable crescent-shaped solitons were predicted in the conservative model of rotating BECs trapped in anharmonic axisymmetric potentials [16].

The above species of the vortices feature stable shapes. On the other hand, in region B of Fig. 1 they are subject to an oscillatory instability, which immediately transforms them into robust *breathers*, which keep the vorticity and axial symmetry. Such stable breathers are similar to the one shown in the first panel of Fig. 6 (the period of its oscillations is $Z \approx 5$). Breathing vortices also appear in region S; however, as shown in Fig. 6, they spontaneously develop

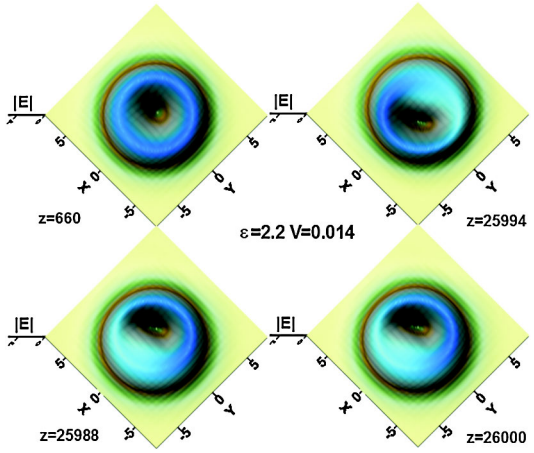

FIG. 5 (color online). The evolution of a stable rotating crescent-shaped vortex.

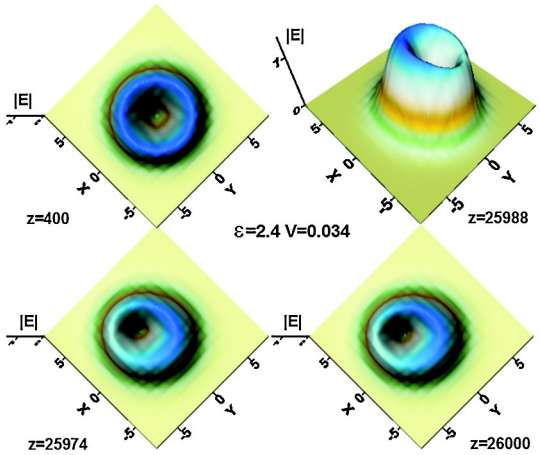

FIG. 6 (color online). A vortex breather formed from the VA-predicted input at $z \simeq 20$ and shown from above at $z = 400$, evolves into an elliptically-shaped "slanted volcano", whose profile is displayed at $z = 25\,988$. It rotates with period $Z \approx 26$ (the images shown at $z = 25\,974$ and $z = 26\,000$ are separated by the period).

the elliptic deformation and cease intrinsic oscillations at $z \simeq 500$. The resulting vortex develops into an elliptic "volcano" which rotates with period $Z \approx 26$. The difference from Fig. 3 is that this vortex species is characterized by the crater which is not undulate but canted.

Conclusion.—Using the variational approximation and numerical simulations, we have developed the analysis of the general 2D model of optical media with the localized linear gain compensated by losses, which models an active part of laser systems. The localized gain provides the stabilization of vortex solitons, which were unstable in previously studied isotropic optical media without diffusion. In addition, stability domains are found for several novel species of vortical solitons, including elliptic spinning ones, double-rotating eccentric vortices, revolving crescents, and breathers. The stabilization mechanism is provided, essentially, by the suppression of the wave field by the growing loss at a large distance from the center, restricting the dynamics to an effectively confined area, where vortices with topological charge $S = 1$ may be stable against splitting [16,17]. This analogy also suggests that all vortices with $S \geq 2$ may be unstable, which requires an additional investigation.

This work was supported, in a part, by the Ministry of Science of Serbia under Project No. OI 141031, and by a grant from the High Council for Scientific and Technological Cooperation between France and Israel. We appreciate valuable discussions with Y. V. Kartashov and V. V. Konotop.

[1] Y. S. Kivshar and G. P. Agrawal, *Optical Solitons: From Fibers to Photonic Crystals* (Academic Press, San Diego, 2003); F. Lederer *et al.*, Phys. Rep. **463**, 1 (2008); Y. V. Kartashov, V. A. Vysloukh, and L. Torner, in *Progress in Optics* (Elsevier B. V., Amsterdam, 2009), Vol. 52, p. 63.

[2] F. T. Arecchi, S. Boccaletti, and P. L. Ramazza, Phys. Rep. **318**, 1 (1999); I. S. Aranson and L. Kramer, Rev. Mod. Phys. **74**, 99 (2002); N. N. Rosanov, *Spatial Hysteresis and Optical Patterns* (Springer, Berlin, 2002); *Dissipative Solitons*, edited by N. Akhmediev and A. Ankiewicz (Springer, Berlin, 2005).

[3] M. Segev *et al.*, Phys. Rev. Lett. **68**, 923 (1992); G. S. Duree *et al.*, *ibid.* **71**, 533 (1993); M. Segev *et al.*, *ibid.* **73**, 3211 (1994); D. N. Christodoulides and M. I. Carvalho, J. Opt. Soc. Am. B **12**, 1628 (1995); V. Skarka, V. I. Berezhiani, and R. Miklaszewski, Phys. Rev. E **56**, 1080 (1997).

[4] B. A. Malomed, Physica (Amsterdam) **29D**, 155 (1987); S. Fauve and O. Thual, Phys. Rev. Lett. **64**, 282 (1990); B. A. Malomed and H. G. Winful, Phys. Rev. E **53**, 5365 (1996).

[5] N. N. Akhmediev, V. V. Afanasjev, and J. M. Soto-Crespo, Phys. Rev. E **53**, 1190 (1996); J. Atai and B. A. Malomed, Phys. Lett. A **246**, 412 (1998); W. J. Firth and P. V. Paulau, Eur. Phys. J. D **59**, 13 (2010).

[6] C.-K. Lam *et al.*, Eur. Phys. J. Special Topics **173**, 233 (2009); C. H. Tsang *et al.*, Eur. Phys. J. D **59**, 81 (2010).

[7] I. V. Barashenkov, N. V. Alexeeva, and E. V. Zemlyanaya, Phys. Rev. Lett. **89**, 104101 (2002); N. V. Alexeeva, Theor. Math. Phys. **144**, 1075 (2005).

[8] V. Skarka, and N. B. Aleksić, Phys. Rev. Lett. **96**, 013903 (2006).

[9] D. Mihalache *et al.*, Phys. Rev. A **75**, 033811 (2007); **77**, 033817 (2008); **81**, 025801 (2010); Phys. Rev. E **78**, 056601 (2008); H. Leblond, B. A. Malomed, and D. Mihalache, Phys. Rev. A **80**, 033835 (2009).

[10] L.-C. Crasovan, B. A. Malomed, and D. Mihalache, Phys. Rev. E **63**, 016605 (2000).

[11] F. Kh. Abdullaev *et al.*, Phys. Rev. A **76**, 043611 (2007); V. A. Brazhnyi *et al.*, Phys. Rev. Lett. **102**, 144101 (2009); Y. V. Bludov and V. V. Konotop, Phys. Rev. A **81**, 013625 (2010); Y. V. Kartashov *et al.*, Opt. Lett. **35**, 1638 (2010).

[12] V. Skarka *et al.*, Phys. Rev. B **81**, 035202 (2010).

[13] C. Rotschild *et al.*, Phys. Rev. Lett. **95**, 213904 (2005).

[14] J. J. García-Ripoll *et al.*, Phys. Rev. Lett. **87**, 140403 (2001); T. J. Alexander, A. A. Sukhorukov, and Y. S. Kivshar, *ibid.* **93**, 063901 (2004); F. Ye, D. Mihalache, and B. Hu, Phys. Rev. A **79**, 053852 (2009); F. Ye *et al.*, J. Opt. Soc. Am. B **27**, 757 (2010).

[15] T. Carmon *et al.*, Phys. Rev. Lett. **87**, 143901 (2001); B. A. Malomed *et al.*, Phys. Rev. A **70**, 043616 (2004); P. Zhang *et al.*, Opt. Lett. **35**, 3129 (2010).

[16] E. Lundh, A. Collin, and K.-A. Suominen, Phys. Rev. Lett. **92**, 070401 (2004); G. M. Kavoulakis, A. D. Jackson, and G. Baym, Phys. Rev. A **70**, 043603 (2004); A. Collin, *ibid.* **73**, 013611 (2006); H. Sakaguchi and B. A. Malomed, *ibid.* **78**, 063606 (2008).

[17] T. J. Alexander and L. Bergé, Phys. Rev. E **65**, 026611 (2002); D. Mihalache *et al.*, Phys. Rev. A **73**, 043615 (2006); L. D. Carr and C. W. Clark, Phys. Rev. Lett. **97**, 010403 (2006).